Mapping of charge density of ion beams produced by laser

J. Krása[1], P. Parys[2], A.Velyhan[1], D. Margarone[1], E. Krouský[1] and J. Ullschmied[3]

[1] *Institute of Physics, ASCR, v.v.i., Prague, Czech Republic*

[2] *Institute of Plasma Physics and Laser Microfusion, Warsaw, Poland*

[3] *Institute of Plasma Physics, ASCR, v.v.i., Prague, Czech Republic*

Abstract — Expansion of ions into vacuum chamber of the 3–TW PALS facility is characterized with ion charge density profiles derived from time-of-flight spectra. The relationship between the charge density profile over path of ions and the time-resolved ion current observed far from the ion source is based on a similarity law for ion currents with "frozen" charges observed at different distances from the target. In this contribution, we present maps of the charge density of ions. These maps demonstrate that jets of ions are emitted at various ejection angles ϕ_n with respect to the target-surface normal.

With the purpose of obtaining information on the space properties of the expanding plasma, several Faraday collectors were located at various angles with respect to the target surface normal. They help to determine angular distributions of various plasma parameters, but their time-resolution is limited due to e.g. time integration of ion currents [1-4]. A new method of transformation of the time-resolved ion currents into the distance-of-flight charge density profiles has been developed in [5, 6]. By separating the ion charge density from the ion current an easy way has been provided to draw the map of ion charge density at a selected time τ after the end of the laser pulse. A set of these maps for various τ visualizes the time development of ion emission if the charge of ions is frozen. The mapping method in question is based on a similarity low for currents of ions with "frozen" charge-states observed far from the target [4]. This similarity law is derived from the signal function, S_x, of an ion collector (IC) positioned on x-axis at a distance L from the target:

$$S_x(L,t) \propto v_x f(\vec{v})\, d\vec{v}\,, \tag{1}$$

where $f(\vec{v})$ is the 3-dimensional velocity distribution function. Substituting L/t into $f(\vec{v})d\vec{v}$ we get the number of particles hitting the detector's area dS per dt, which is proportional to $f(L/t)\, L\, t^{-4}$ and $S_x(L,t) \sim L^2\, t^{-5}\, f(L/t)\, dtdS$. Taking into consideration that $t = L/v$, the relationship (1) takes the following form for the ion current [5.6]:

$$j(L,t)\, L^3 = \kappa\, v^5\, f(v). \tag{2}$$

Then the similarity law for current densities of ions with "frozen" charges, which are detected at different distances x and L, reads:

$$j(x,\tau)\, x^3 = j(L,t)\, L^3 , \tag{3}$$

where $x/\tau = L/t$. This similarity law allows us to determine the space-resolved ion charge density $q = j/v$ by using the transformation of the time-of-flight spectrum $j(L,t)$ to the distance-of-flight spectrum (DOF) $q(x,\tau)$, where the flight times t, τ are related into the flight distances L, x as $L/t = x/\tau$. Dividing (3) by x/τ, we obtain the DOF spectrum [5]:

$$q(x,\tau) = j(L, \tau L/x)\ \tau L^3/x^4, \tag{4}$$

where the time τ is a parameter.

The plasma produced with the laser intensity of 10^{16} W/cm^2 emits three basic groups of ions: thermal, fast, and superfast groups expanding into vacuum with velocity of 10^{-5}, 10^{-6}, and 10^{-7} m/s, respectively. The thermal ions are those generated indirectly around the laser focus spot by X–rays from the hot plasma and the superfast group may be ascribable to self-focusing of the laser beam [7]. The fast and superfast ion groups are shown in Fig. 1. The ion current density was measured with the use of an IC positioned 134 cm far from a CD_2 target foil of 500 μm in thickness. The laser beam was focused onto the target at an angle of 30° with respect to the target surface normal while the IC collected ions along the target normal in the backward direction with respect to the laser beam. The highest value of the current density was reached by the superfast ions expanding with velocity $v_i > 1\times10^7$ m/s (see Fig. 1a). However, the group of fast ions has higher charge density, as Fig. 1b shows. The highest value of the charge density belongs to the group of slow thermal ions, as shown in Fig. 2.

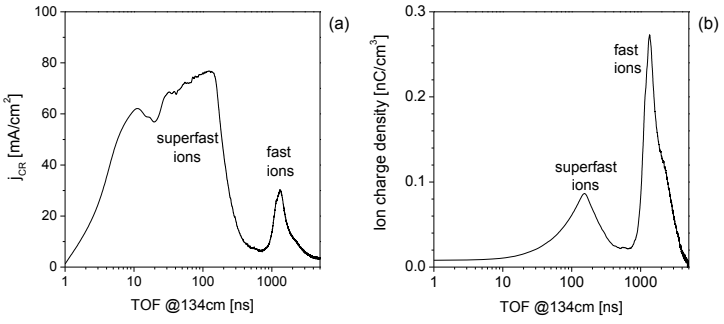

Fig. 1. Current density of ions emitted by deuterated polyethylene plasma (a) and corresponding ion charge density (b) observed at a distance of 134 cm far from the target.

Applying the relationship (4), the time-resolved ion current density (see Fig. 1a) can be transformed in the DOF spectrum for a chosen time τ after the end of the laser pulse, as Fig. 2 shows for $\tau = 100$ and 1000 ns. It is obvious that all the three groups of ions occupy the

150 cm long path from the target at $\tau = 100$ ns. The slow thermal ions possess the highest charge density. The charge density of all the ion groups rapidly decreases with increasing the distance from the target (it is by about 6 orders of magnitude lower at the distance of 150 cm from the target at $\tau = 100$ ns). The DOF spectrum has only one maximum that belongs to the thermal ions, contrary to the TOF spectrum, which has three well separated ion groups (only two of them being shown in Fig. 1). In general, the other maxima are transformed into inflex points of the DOF spectrum. This is caused by the strong decrease in the charge density according to the relation $q(x,\tau) \sim x^{-4}$.

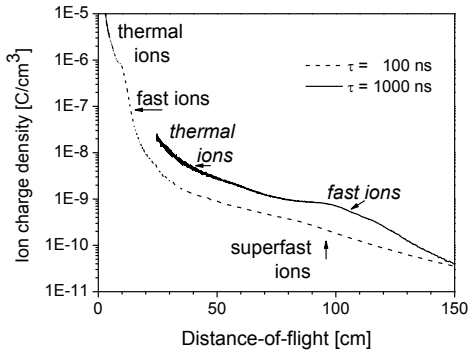

Fig. 2. DOF spectrum of ion charge density at 100 and 1000 ns after the end of laser pulse which was derived from the IC signal shown in Fig. 1a using the formula (4).

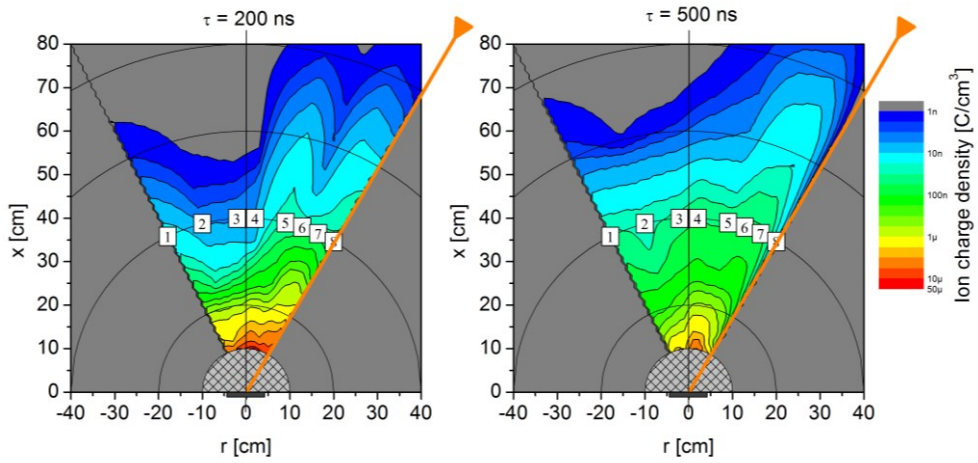

Fig. 3. Charge density map of deuterons and carbon ions 200 and 500 ns after the end of the laser pulse. The labels indicate the directions of observation of ion currents with the use of eight Faraday cups positioned 40 cm far from the $(CD_2)_n$ target. The laser beam struck the target with 30° incidence angle; the intensity on target was 3×10^{16} W/cm^2 (shot #40209, E_L=535 J, λ=1315 μm, focus position is 100 μm in front of the target surface).

Simultaneous observations of TOF spectra in different directions allowed us to determine the dependence of the ion emission on the angle related to the target normal. We used 8 Faraday cups (FC) positioned at various angles of observation. Using the formula (4) we obtain a map of ion charge density for a chosen time from the laser-target interaction, as Fig. 3 shows for $\tau = 200$ and 500 ns. This map demonstrates the asymmetry in ion charge density distribution

with respect to the target surface normal, as well as the enhanced density in the direction of laser beam. The ion charge density map drawn for $\tau = 200$ ns shows that the fastest ions are ejected in the direction of 13° with respect to the target normal (FC–5), while the map drawn for a later time, $\tau = 500$ ns, shows that the slower ions expand at ejection angles of –24° (FC–1), and 24° (FC–7).

In conclusion, we have determined experimentally the angularly resolved charge density maps of ions for various times after the end of the laser pulse. They demonstrate that the ion stream, composed of slow thermal, fast, and superfast groups, is divided into partial jets flying in different directions with respect to the target surface normal. Individual ion groups are produced and accelerated by various different mechanisms. Thus, we can conclude that the plasma expands in a form of a multi-jet fountain, in which where the central jet expands closely along the target surface normal, the others exhibiting an increasing declination from the central one.

Acknowledgement

The research leading to these results has received funding from the Czech Science Foundation (Grant No. P205/12/0454), the Czech Republic's Ministry of Education, Youth and Sports (Project No. LM2010014), the LASERLAB-EUROPE (Grant Agreement No. 284464, EC's Seventh Framework Programme), the Academy of Sciences of the Czech Republic (Project No. M100101210), and the European Social Fund and the state budget of the Czech Republic (Project No. CZ.1.07/2.3.00/20.0279).

References

[1] A. Thum, A. Rupp, K. Rohr, J. Phys. D: Appl. Phys. **27** (1994) 1791-1794.

[2] A. Thum-Jäger, K. Rohr, J. Phys. D: Appl. Phys. **32** (1999) 2827–2831.

[3] L. Láska, K. Jungwirth, J. Krása, E. Krouský, M. Pfeifer, K. Rohlena, A. Velyhan, J. Ullschmied, S. Gammino, L. Torrisi, J. Badziak, P. Parys, M. Rosinski, L. Ryć, J. Wolowski. Laser. Part. Beams **26** (2008) 555-565.

[4] J. Krása, A. Lorusso, V. Nassisi, L. Velerdi, A. Velyhan. Laser. Part. Beams **29** (2011) 113-119.

[5] J. Krása, P. Parys, L. Velardi, A. Velyhan, L. Ryć , D. Delle Side, V. Nassisi. Laser Part. Beams **32** (2014) 15-20.

[6] J. Krása, L. Velardi, A. Lorusso, D. Delle Side, V. Nassisi. J. Phys. Conf. Series **508** (2014) 012004.

[7] L. Láska, K. Jungwirth, B. Králiková, J. Krása, M. Pfeifer, K. Rohlena, J. Skála, J. Ullschmied, J Badziak, P. Parys, J. Wolowski, E. Woryna, S. Gammino, L. Torrisi, F. P. Boody, H. Hora. Plasma Phys. Control. Fusion **45** (2003) 585–599.